Civil Engineering   School of Engineering

Uncertainty in projections of streamflow changes due to climate change in California

Edwin P. Maurer
Santa Clara University, emaurer@scu.edu

Philip B. Duffy

Follow this and additional works at: https://scholarcommons.scu.edu/ceng

Part of the Civil and Environmental Engineering Commons

Uncertainty in projections of streamflow changes due to climate change in California

Edwin P. Maurer[1] and Philip B. Duffy[2]

[1]   Understanding the uncertainty in the projected impacts of climate change on hydrology will help decision-makers interpret the confidence in different projected future hydrologic impacts. We focus on California, which is vulnerable to hydrologic impacts of climate change. We statistically bias correct and downscale temperature and precipitation projections from 10 GCMs participating in the Coupled Model Intercomparison Project. These GCM simulations include a control period (unchanging CO_2 and other forcing) and perturbed period (1%/year CO_2 increase). We force a hydrologic model with the downscaled GCM data to generate streamflow at strategic points. While the different GCMs predict significantly different regional climate responses to increasing atmospheric CO_2, hydrological responses are robust across models: decreases in summer low flows and increases in winter flows, and a shift of flow to earlier in the year. Summer flow decreases become consistent across models at lower levels of greenhouse gases than increases in winter flows do. **Citation:** Maurer, E. P., and P. B. Duffy (2005), Uncertainty in projections of streamflow changes due to climate change in California, *Geophys. Res. Lett.*, *32*, L03704, doi:10.1029/2004GL021462.

1.   Introduction

[2]   Global climate change, largely human induced in recent decades [e.g., *Meehl et al.*, 2004], will result in a warmer environment, with associated regional impacts [*Karl and Trenberth*, 2003]. Changes in the hydrologic cycle will provide both positive feedback to warming trends and a principal avenue for humans to tangibly experience the regional effects of global climate change [*Houghton et al.*, 2001]. Considerable uncertainty remains in estimating the impacts due to projected climate changes, which is attributed to both uncertainty in the future emissions pathway (related to policy decisions and public response) and uncertainties in model projections (due to differing model sensitivities to perturbations in atmospheric composition); the latter is the focus of this study. These uncertainties are of comparable magnitude on a global scale [*Karl and Trenberth*, 2003; *Wigley and Raper*, 2001], though for any particular region they may not be. While there is a need to explore the probabilistic character of future climate states by developing multiple ensembles of projected climate

[*Houghton et al.*, 2001], only recently have these differing sources of uncertainty been examined separately [*Hayhoe et al.*, 2004].

[3]   California is an interesting case study for examining the hydrologic impacts of climate change, being highly dependent on both the amount and timing of seasonal snow accumulation and melt [*VanRheenan et al.*, 2004], and thus vulnerable to changes in either temperature (T) or precipitation (P). California has been the focus of many previous studies on hydrologic effects of climate change, using different techniques to ingest global climate model (GCM) data into hydrologic models. Recent examples include statistical downscaling of multiple emissions scenarios with one GCM [*VanRheenan et al.*, 2004; *Dettinger et al.*, 2004] or two GCMs [*Hayhoe et al.*, 2004], perturbing historical climate with plausible shifts [*Miller et al.*, 2003], dynamically downscaling a GCM [*Kim*, 2005] and using a regional climate model under a mean state of doubled CO_2 [*Snyder et al.*, 2002]. While these provide valuable information on the range of possible hydrologic impacts of climate change on California, none can adequately assess the uncertainty in the estimates. What this study presents is a quantification of the uncertainty due to using different GCMs (and to sampling 20-year periods of their output) to estimate streamflow impacts in California.

2.   Methods

[4]   The GCMs selected for this study are the 10 models that participated in the most recent phase of the Coupled Model Intercomparison Project (CMIP) [*Covey et al.*, 2003; *Meehl et al.*, 2000] and that provided atmospheric data. These are listed in Table 1, and are described further in the CMIP web site (www-pcmdi.llnl.gov/projects/cmip/).

[5]   GCM P and T output was bias-corrected and statistically downscaled to a 1/8° grid (~150 km^2). Downscaling to the 1/8° grid used an empirical statistical technique that maps the probability density functions for the monthly GCM P and T for the first 40 years of the GCM control simulation (in which CO_2 and other external control forcing are kept constant) onto those of gridded historical observed data for 1960–1999, so the mean and higher moments of observations are reproduced by the control climate model data. This same mapping is applied to an additional 20 years (years 41–60) of control simulation, and then to 70 years of "perturbed" GCM simulations, where CO_2 increases by 1% per year. (At 70 years, a 1%/year increase doubles the control level CO_2). This allows the mean and variability of each GCM to evolve in accordance with the simulation, while matching all statistical moments between the GCM control period and the 1960–1999 observed period. The bias correction (and spatial disaggregation) technique is one

[1]Civil Engineering Department, Santa Clara University, Santa Clara, California, USA.
[2]Atmospheric Science Division, Lawrence Livermore National Laboratory, Livermore, California, USA.

Table 1. GCM Simulations Used in This Study

Abbrev.	Model, Year	Sponsor
CCCMA	CCCMA, 2001	Canadian Centre for Climate Modelling and Analysis
CSIRO	CSIRO_Mk2, 1997	Commonwealth Scientific & Industrial Research Organization
GFDL	GFDL_R30_c, 1996	Geophysical Fluid Dynamics Laboratory
HadCM2	HadCM2, 1995	UK Meteorological Office
HadCM3	HadCM3, 1997	UK Meteorological Office
MD	ECHO-G, 1999	Model & Data Group (Germany)
MPI	ECHAM4_OPYC3, 1996	Max Planck Institut fur Meteorologie
MRI	MRI_CGCM2.3, 2002	Meteorological Research Institute (Japan)
NCAR	CCSM2.0, 2002	National Center for Atmospheric Research
PCM	PCM, 1999	Department of Energy (USA)

originally developed for adjusting GCM output for long-range streamflow forecasting [*Wood et al.*, 2002] that was later adapted for use in studies examining the hydrologic impacts of climate change [*VanRheenan et al.*, 2004]. While the technique does not account for changes in the statistics of climate variability at scales less than monthly, it has compared favorably to different statistical and dynamic downscaling techniques [*Wood et al.*, 2004] in the context of hydrologic impact studies. The downscaled data is used to force the Variable Infiltration Capacity model using the identical parameterization as *VanRheenan et al.* [2004] to be able to isolate the hydrologic response of a suite of GCMs under identical CO_2 concentrations.

[6] A second experiment is performed using the T forcing from the 10 GCMs, but for all GCMs replacing the P with the (bias corrected, downscaled) P from the PCM run, which shows the greatest correspondence each season to climatological P and is the least sensitive to increasing CO_2. The fraction of the streamflow variability attributable to differing GCM P is computed according to equation (1).

$$Fraction = \frac{\sigma_{TP} - \sigma_T}{\sigma_{TP}} \qquad (1)$$

where σ is the standard deviation (SD) of streamflow produced by the GCMs, T and TP indicate T or both T and P, respectively, vary between all GCMs. While the resulting sequences of P and T fail to preserve the physical relationship between them in a GCM, this P substitution allows the estimation of the amount of inter-model variability in hydrologic impacts attributable to P and T individually.

3. Results and Discussion

[7] We focus on the Sacramento-San Joaquin Basin, shown in Figure 1. The three northern gauges are considered together, as are the four southern gauges, all of which are inflows to major reservoirs and which together account for most of the Sacramento-San Joaquin streamflow originating from the Sierra Nevada mountains. In general, the southern area drains a greater proportion of higher elevation area than the North, and thus has been shown to respond differently to climate change [*Knowles and Cayan*, 2004].

[8] Figure 2 shows the simulated streamflow for the North and South, showing the characteristic snowmelt-driven annual hydrograph, and the later melt and hydrograph peak for the South. Figures 2a and 2d show for the control period years 41–60 the inter-model variability

introduced by sampling a 20-year slice of time not used in the bias correction, with variability being due to longer time-scale departures of models occurring at different times. Though not shown, using years 21–40 of the control period (included in the bias correction training) produces about half the variability of years 41–60. For July–November variability is small and close to the variability in perturbed years. During winter months the variability is substantially smaller than during the perturbed period, showing inter-model variability in winter is largely due to differing GCM responses to future forcing, especially in later years.

[9] The changes in flow are driven by an average increase, across GCMs, in annual P of 2% and 7% for perturbed years 21–40 and 51–70, respectively, with sharpest increases in winter, at 6% and 13%. The accompanying average T rises 1.1 and 2.2°C for the earlier and later perturbed periods, respectively, with summer T rising slightly more than winter, at 1.3 and 2.7°C. These basin-wide changes are nearly identical in the North and South.

[10] Figures 2b and 2e show that inter-model variation appears within the first few decades, and Figures 2c and 2f show that uncertainty increases somewhat during later
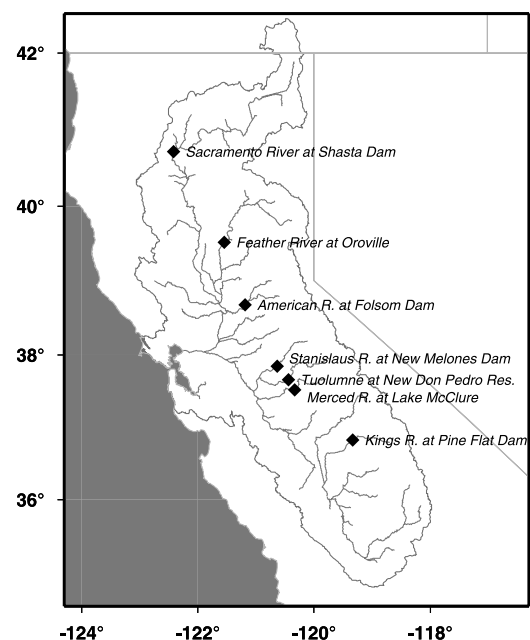

Figure 1. Sacramento-San Joaquin basin, the region included in this study, with 3 northern and 4 southern stream gauges.
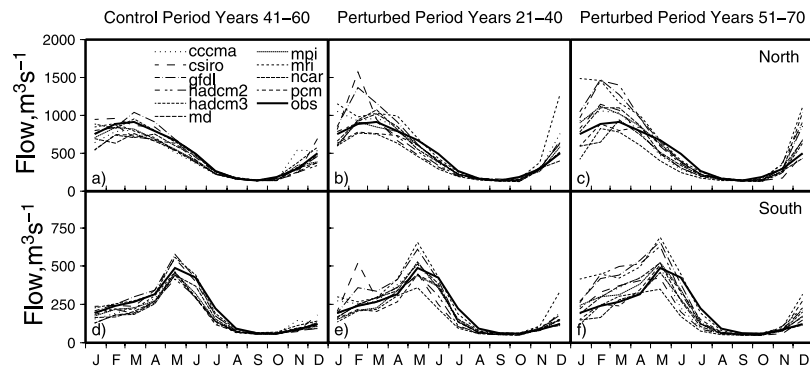
Figure 2. Streamflow simulations forced by the 10 GCMs for the North 3 gauges (top 3 panels) and the South 4 gauges (bottom 3 panels). a) and d) Control years 41–60, b) and e) Perturbed years 21–40, c) and f) Perturbed years 51–70. The ''obs'' line, repeated for reference on all panels, shows the hydrograph for the 1960–1999 period, which is the benchmark period to which the control period GCM output was bias-corrected.

periods, in months at and before the annual hydrograph peak. Table 2 shows that by years 21–40 the decrease in late spring and early summer flows in the North is significant, with the change in mean flow exceeding the inter-model variability at greater than a 90% confidence level. By years 51–70, the increase in winter and decrease in summer flows are both significant. November, January, and May are least significant, which, for November and May shows higher uncertainty during transition periods (at the beginning and end of the rainy season).

[11] Table 3 shows for the South uncertainty in changes in spring flows remains low (except in May). The increase in March–April flows is more highly significant than in North, and reaches significance levels over 90% earlier, by years 21–40. This shows the greater influence in the higher altitude (hence more snow dominated) South of projected temperature changes, which are more consistent between GCMs (as will be demonstrated below). As in the North, November and May, as transition months, show low significance in change in streamflow from control period, indicating greater inter-model variation relative to change in mean.

[12] Table 4 shows the high confidence in the shift to earlier dates for the peak in the annual hydrograph

(calculated using the center-of-mass approach of *Stewart et al.* [2004]). This shows that 51–70 years into the perturbed run, the annual hydrograph will shift 11 days earlier in the North and 18 days earlier in the South, and that this is very robust across models.

[13] Table 5 shows the results of the second experiment, where an identical P sequence was used for all GCMs. Inter-model variation in projected P accounts for 72–90% of the total inter-model variation in October–February flow increases. Inter-model P variability is substantially more dominant than T variability for streamflow uncertainty except during May–July in the North and June–August in the South, especially for the earlier years 21–40 of the perturbed run, reflecting lessened impact during the dry season. While rising T drives the pattern of earlier snowmelt and the shifting of the annual hydrograph to earlier in the year (hence low uncertainty in these impacts), P largely determines the magnitude of monthly streamflow change outside of the summer low flow periods. In June, uncertainty in streamflow projections due to inter-model P variability grows later in the perturbed period, indicating a divergence of the GCMs. Table 5 shows the distinction between North and South, especially in March–April where the influence of P is less in the South, thus greater T-driven

Table 2. Streamflow Statistics for the Composite Hydrograph of the Three North Gauges, Calculated Across Different GCMs, Quantifying the Degree of Consistency Between GCM Results[a]

Control 1–40		Perturbed 21–40				Perturbed 51–70			
Month	Mean	Mean	SD	CV	1-tprob %	Mean	SD	CV	1-tprob %
1	717	777	197	0.25	63.9	855	296	0.35	75.1
2	861	1008	259	0.26	89.1	1118	285	0.25	93.7
3	875	947	132	0.14	87.4	1059	193	0.18	96.5
4	764	795	112	0.14	58.9	842	120	0.14	83.6
5	609	572	73	0.13	84.4	554	90	0.16	83.8
6	436	373	44	0.12	99.8	342	52	0.15	99.8
7	246	220	18	0.08	99.8	213	23	0.11	99.5
8	169	161	8	0.05	99.1	157	10	0.06	98.3
9	142	141	8	0.05	44.2	139	5	0.04	77.5
10	156	145	17	0.12	93.1	143	11	0.08	92.7
11	287	299	32	0.11	73.0	276	58	0.21	36.3
12	508	650	244	0.38	89.9	775	229	0.3	96.7

[a]Mean and standard deviation (SD) are in m^3/s, tprob is the probability (according to a 2-tailed t-test for differences in mean) of claiming the perturbed mean is different from the control mean when they are actually the same. Thus, 1-tprob is the confidence level that the perturbed mean is different from the control. (Note that the probability of the perturbed distribution containing the control mean would be lower). CV is the coefficient of variation, (standard deviation over the mean).

Table 3. Same as Table 2, but for the Composite Hydrograph of the Southern Gauges

Control 1−40		Perturbed 21−40				Perturbed 51−70			
Month	Mean	Mean	SD	CV	1-tprob %	Mean	SD	CV	1-tprob %
1	172	195	54	0.28	78.4	226	85	0.38	87.7
2	225	278	96	0.34	88.8	321	94	0.29	95.0
3	241	270	41	0.15	93.9	361	79	0.22	99.8
4	298	351	46	0.13	99.4	418	77	0.18	99.8
5	482	497	87	0.18	40.1	526	107	0.2	66.3
6	389	345	67	0.19	92.8	300	85	0.28	97.2
7	167	136	27	0.2	99.3	122	34	0.28	99.0
8	75	68	6	0.09	99.4	64	7	0.11	99.6
9	60	56	5	0.08	94.6	54	3	0.06	99.3
10	60	56	4	0.08	98.5	53	4	0.08	99.3
11	86	92	10	0.11	88.7	83	13	0.16	41.8
12	134	175	64	0.36	92.4	207	59	0.29	97.2

Table 5. Percent of Inter-model Variability in Monthly Streamflow for the Composite North and South Hydrographs Attributable to Inter-model Variability in Precipitation[a]

	North, %		South, %	
Month	Perturbed 21−40	Perturbed 51−70	Perturbed 21−40	Perturbed 51−70
1	90	91	90	90
2	78	76	77	74
3	81	84	70	69
4	77	67	40	72
5	43	52	69	63
6	24	48	35	60
7	48	54	49	54
8	57	61	52	38
9	74	57	66	39
10	91	84	72	72
11	83	97	75	86
12	90	84	88	82

[a]The remainder is attributable to inter-model temperature variability.

impacts in the South. For September streamflows, inter-model P variability is generally less important in the later period than in the early period, suggesting that as T continues to rise, the differences in GCM projected P have less of an effect on late dry season streamflow. One explanation would be that as snowmelt occurs earlier and P falls more frequently as rain than snow due to rising T, the ability of the lagging effects of water storage in snow (and soil moisture) to carry P anomalies late into the wet season may decline.

4. Conclusions

[14] We examined the effects of variability of GCM output on simulated streamflow in the Sacramento-San Joaquin basin in California. Uncertainty in streamflow impacts due to inter-model variability between the 10 GCMs considered here does not prevent significant detection of decreases in summer flows even after 21−40 years of 1% per year increasing CO_2. Both increases in winter and decreases in summer streamflows are robust by years 51−70, with the projected changes significantly exceeding the inter-model variability. The retreat of the midpoint of annual runoff volume to earlier in the season is also very robust across GCMs. The inter-model variability produces the greatest uncertainty in transition months at beginning and end of rainy season, where the projected streamflows using different GCMs show greater variability.

[15] Uncertainty due to sampling of a 20-year period in an extended GCM simulation accounts for the majority of inter-model variability for summer and fall months, while varying GCM responses to T and P forcing add to the variability in the winter. Inter-model variation in projected

P accounts for most of the uncertainty in winter and spring flow increases in both the North and South regions, with a greater influence in the North. Thus, streamflow impacts in the higher elevation (and more snow dominated) South tend to be more T-driven, and hence to have less uncertainty. The influence of inter-model P variability on late summer streamflow decreases in later years, as higher Ts dominate the hydrologic response, and melting snowpack has less influence. Conversely, the contribution of GCM P variability to early summer streamflow uncertainty increases later in the perturbed period.

References

Covey, C., K. M. AchutaRao, U. Cubasch, P. Jones, S. J. Lambert, M. E. Mann, T. J. Phillips, and K. E. Taylor (2003), An overview of results from the Coupled Model Intercomparison Project (CMIP), *Global Planet. Change*, *37*, 103–133.

Dettinger, M. D., D. R. Cayan, M. K. Meyer, and A. E. Jeton (2004), Simulated hydrologic responses to climate variations and change in the Merced, Carson, and American River basins, Sierra Nevada, California, 1900–2099, *Clim. Change*, *62*, 283–317.

Hayhoe, K., et al. (2004), Emissions pathways, climate change, and impacts on California, *Proc Natl. Acad. Sci. U. S. A.*, *101*, 12,422–12,427.

Houghton, J. T., Y. Ding, D. J. Griggs, M. Noguer, P. J. van der Linden, X. Dai, K. Maskell, and C. A. Johnson (Eds.) (2001), *Climate Change 2001: The Scientific Basis: Contribution of Working Group I to the Third Assessment Report of the Intergovernmental Panel on Climate Change*, 881 pp., Cambridge Univ. Press, New York.

Karl, T. R., and K. E. Trenberth (2003), Modern global climate change, *Science*, *302*, 1719–1723.

Kim, J. (2005), A projection of the effects of the climate change induced by increased CO_2 on extreme hydrologic events in the western U.S., *Clim. Change*, in press.

Knowles, N., and D. R. Cayan (2004), Elevational dependence of projected hydrologic changes in the San Francisco estuary and watershed, *Clim. Change*, *62*, 319–336.

Meehl, G. A., G. J. Boer, C. Covey, M. Latif, and R. J. Stouffer (2000), The Coupled Model Intercomparison Project (CMIP), *Bull. Am. Meteorol. Soc.*, *81*, 313–318.

Meehl, G. A., W. M. Washington, C. M. Ammann, J. M. Arblaster, T. M. L. Wigley, and C. Tebaldi (2004), Combinations of natural and anthropogenic forcings in 20th century climate, *J. Clim.*, *17*, 3721–3727.

Miller, N. L., K. E. Bashford, and E. Strem (2003), Potential impacts of climate change on California hydrology, *J. Am. Water Resour.Assoc.*, *39*, 771–784.

Table 4. Statistical Comparison of the Day of Year to the Centroid of the Annual (Water Year) Runoff Hydrograph[a]

	Control Period	Perturbed 21−40				Perturbed 51−70			
Statistic	Mean	Mean	SD	CV	1-tprob %	Mean	SD	CV	1-tprob %
Day of year to runoff centroid: North	74	67	7	0.11	98.4	63	7	0.11	99.9
Day of year to runoff centroid: South	119	110	9	0.08	99.4	101	7	0.07	100

[a]See Table 2 for column definitions.

Snyder, M. A., J. L. Bell, L. C. Sloan, P. B. Duffy, and B. Govindasamy (2002), Climate responses to a doubling of atmospheric carbon dioxide for a climatically vulnerable region, *Geophys. Res. Lett.*, *29*(11), 1514, doi:10.1029/2001GL014431.

Stewart, I. T., D. R. Cayan, and M. D. Dettinger (2004), Changes in snowmelt runoff timing in western North America under a 'business as usual' climate change scenario, *Clim. Change*, *62*, 217–232.

VanRheenan, N. T., A. W. Wood, R. N. Palmer, and D. P. Lettenmaier (2004), Potential implications of PCM climate change scenarios for Sacramento–San Joaquin River basin hydrology and water resources, *Clim. Change*, *62*, 257–281.

Wigley, T. M. L., and S. C. B. Raper (2001), Interpretation of high projections for global-mean warming, *Science*, *293*, 451–454.

Wood, A. W., E. P. Maurer, A. Kumar, and D. P. Lettenmaier (2002), Long-range experimental hydrologic forecasting for the eastern U.S., *J. Geophys. Res.*, *107*(D20), 4429, doi:10.1029/2001JD000659.

Wood, A. W., L. R. Leung, V. Sridhar, and D. P. Lettenmaier (2004), Hydrological implications of dynamical and statistical approaches to downscaling climate model outputs, *Clim. Change*, *62*, 189–216.

————————————

P. B. Duffy, Atmospheric Science Division, Lawrence Livermore National Laboratory, Livermore, CA 94551–0808, USA. (pduffy@llnl.gov)

E. P. Maurer, Civil Engineering Department, Santa Clara University, Santa Clara, CA 95053–0563, USA. (emaurer@scu.edu)